

Magnetic Ordering in Organic-Radical Assemblies. II[1]

Masashi Hatanaka* and Ryuichi Shiba

Department of Materials and Life Sciences, Graduate School of Advanced Science & Technology, Tokyo Denki University, 2-2 Kanda Nishiki-cho, Chiyoda-ku, Tokyo 101-8457

Received August 15, 2008; E-mail: mhatanaka@xug.biglobe.ne.jp

Intermolecular distance dependence on ferromagnetic interactions in organic-radical assemblies was deduced by using molecular orbital methods. It was shown that non-bonding molecular orbitals (NBMOs) were subject to orbital mixing to form localized NBMOs. The high-spin stabilities had maxima when magnitude of intra- and intermolecular resonance integrals was nearly equal. From amplitude pattern analysis of NBMOs, the origin of the maxima was attributed to itinerant character of the non-bonding electrons in the proper intermolecular distance regions. Our analysis was supported by theoretical calculations.

Ferromagnetic interactions in three-dimensionally stacked organic-radical assemblies have been interpreted in view of spin-polarization concepts, which have been pointed out by McConnell.[2] The McConnell model is based on the Heisenberg Hamiltonian:[2]

$$H^{AB} = -\boldsymbol{S}^{A}\cdot\boldsymbol{S}^{B}\sum_{i,j} J_{ij}^{AB}\sigma_i^{A}\sigma_j^{B} \quad (J_{ij}^{AB} < 0) \tag{1}$$

where $\boldsymbol{S}^{A}$ and $\boldsymbol{S}^{B}$ are spin operators of molecule A and B, respectively, and J_{ij}^{AB} is the exchange integral. We note that J_{ij}^{AB} is negative, analogous to conventional valence bond theory.[3] σ_i^{A} and σ_j^{B} are spin densities at the i-th site in molecule A and the j-th site in molecule B, respectively. That is, spatially stacked spin-polarized π systems are predicted to be ferromagnetic when spin density products become as negative as possible. Then, the expectation value of the Hamiltonian in eq 1 is minimized, and thus, spin polarization is induced at each adjacent carbon atomic site in organic-radical assemblies. In McConnell's model, each spin is localized at one atom, because the formulation is based on valence bond theory. Therefore, in this model, the magnetic orderings are determined by whether or not ferrimagnetism-like spin-polarization structure can be drawn. Indeed, many organic ferromagnets have been suggested by applying the spin-polarization rule.[4–6]

1 in Figure 1 is the simplest example of a high-spin organic-radical assembly, that is, allyl-radical dimer. This supermolecule has been theoretically predicted to be a ground-state triplet.[4] The carbon atom sites are divided into two groups, that is, starred atoms and unstarred atoms, which are not adjacent to each other similar to non-Kekulé molecules.[1] One can draw a spin-polarization structure with high-spin ground state, as shown in Figure 1. Up and down spins are induced on starred and unstarred atoms, respectively. **2** in Figure 2 is pseudo-*para*-benzyl dimer, of which derivative pseudo-*p*-bis(phenylmethylenyl)[2.2]paracyclophane (**3** in Figure 2) was experimentally characterized as a ground-state quintet.[7–9] The spin-polarization structure of **2** is also drawn in Figure 2. Similarly, **4** in Figure 3 is pseudo-*ortho*-benzyl dimer, of which derivative pseudo-*o*-bis(phenylmethylenyl)[2.2]paracyclophane (**5** in Figure 3) was also experimentally characterized as a ground-state quintet.[7–9] The spin-polarization structure of **4** is also drawn in Figure 3. Thus, the spin-polarization mechanism

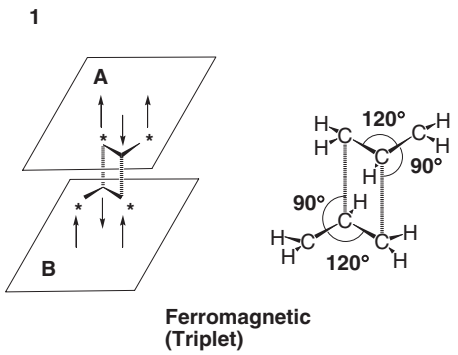

Figure 1. Molecular structure and spin polarization of an allyl-radical assembly **1**. The conformational parameters are also shown.

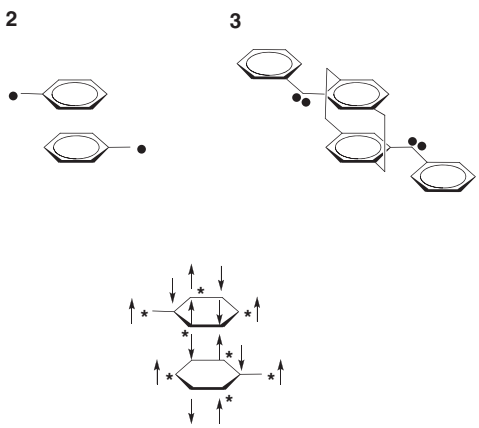

Figure 2. Molecular structures of pseudo-*para*-benzyl dimer **2** and pseudo-*p*-bis(phenylmethylenyl)[2.2]paracyclophane (**3**).

Published on the web February 13, 2009; doi:10.1246/bcsj.82.206

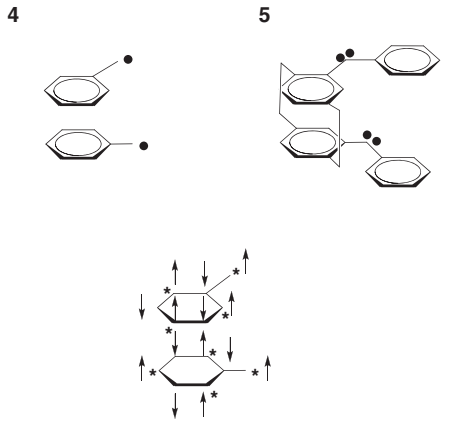

Figure 3. Molecular structures of pseudo-*ortho*-benzyl dimer **4** and pseudo-*o*-bis(phenylmethylenyl)[2.2]paracyclophane (**5**).

has been regarded as the essential origin of high-spin stabilities in organic-radical assemblies. Theoretical aspects of the spin-polarization rule in diphenylcarbenes including **3** and **5** have been rationalized to UHF (unrestricted Hartree–Fock) wave functions, in which spin densities with plus and minus signs are well calculated.[4–6,10] The mechanism has been complemented by molecular orbital methods in view of non-overlapping interactions of the degenerate SOMOs (single occupied molecular orbitals) and Hund's rule.[11,12]

Recently however, we find that organic-radical assemblies can be regarded as extended non-Kekulé systems in that their magnetic properties are determined by topology of the carbon atom linkage. That is, three-dimensionally stacked organic-radical assemblies have degenerate non-bonding molecular orbitals (NBMOs), and thus, high-spin stabilities result from the exchange integral between the NBMOs.[1] In the case of periodic systems, we can construct non-bonding crystal orbitals (NBCOs) instead of NBMOs. Then, NBMOs or NBCOs should be localized as much as possible to form unitary- or Wannier-transformed orbitals, which minimize the exchange integral.[1] These situations resemble those in the so-called disjoint/nondisjoint concept, which has been introduced by Borden and Davidson.[13] That is, whereas NBMOs in singlet biradicals can be made to span no common atoms, which is disjoint type, NBMOs in triplet biradicals can be made to span common atoms, which is nondisjoint type.[13,14] It is important that degenerate orbitals are uniquely determined by unitary- or Wannier transformation so as to minimize the exchange integral. A unitary-transformation procedure has been introduced by Aoki and Imamura,[15] and applied for analysis of high-spin polyradicals.[16,17] Through space interactions in non-Kekulé biradicals have also been analyzed by using the unitary-transformation procedure.[18] The Wannier transformation has been introduced in our previous work,[19,20] and applied for analysis of polymer ferromagnets.[1,19,20] In these treatments, the exchange integral results from antiparallel-spin instabilities due to the Coulomb repulsion in the common spanned atomic orbitals.[1,18–20] The essential origin of high-spin stabilities in organic-radical assemblies has been well described by our analysis rather than conventional spin-polarization rules. Indeed, antiferromagnetic behaviors in some organic-radical

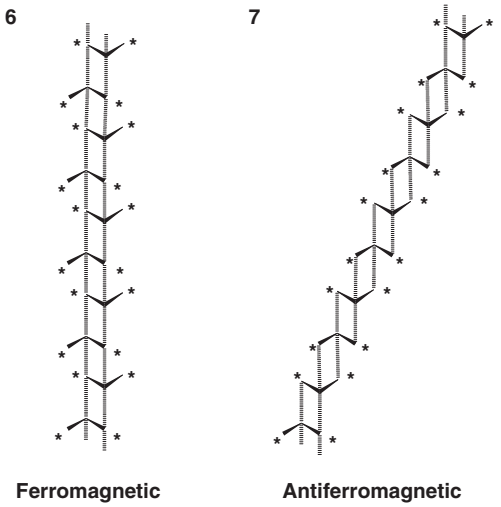

Figure 4. Molecular structures of poly-allyl-radical assemblies. **6** is ferromagnetic and **7** is antiferromagnetic.

assemblies have been well explained by highly localized NBCOs, even if the spin-polarization structures suggest high-spin ground states. For example, Figure 4 shows two allyl-radical assemblies **6** and **7**, of which starred- and unstarred-atom linkages predict high-spin ground states. That is, if up and down spins are induced on starred and unstarred atoms, respectively, both **6** and **7** are intuitively expected to be ferromagnetic. Nevertheless, localized-NBCO analysis and density-functional-theory calculations predicted a ferromagnetic ground state of **6** and an antiferromagnetic ground state of **7**.[1] Instead of the spin-polarization rule, whether or not the Wannier transformed NBCOs are delocalized over more than one unit cell has distinguished the magnetic properties in these organic-radical assemblies.[1] That is, whereas Wannier transformed NBCOs of **6** are delocalized over more than one unit cell, Wannier transformed NBCOs of **7** are localized only at one unit cell.[1] Thus, exchange integral in **6** is positive due to the common spanned atoms.[1] On the other hand, exchange integral in **7** is theoretically zero due to the absence of common spanned atoms.[1] We think that localized orbitals such as unitary-transformed NBMOs or Wannier transformed NBCOs play an essential role in determining the magnetic characteristics in organic-radical assemblies. The localized orbital method rather than the conventional spin-polarization rule seems to be a promising principle for description of magnetic properties in organic ferromagnets.

In this paper, we show intermolecular-distance dependence on the exchange integral of organic-radical assemblies by analyzing allyl, pseudo-*para*-benzyl, and pseudo-*ortho*-benzyl dimers. We regard these radical assemblies as extended non-Kekulé systems, because they are topologically akin to so-called non-disjoint systems, which have linking points between the starred atoms and unstarred atoms. We construct NBMOs by conventional Hückel-like secular equations, and transform the canonical NBMOs into maximally localized NBMOs. The resultant exchange integrals were plotted versus the intermolecular distances. It was shown that high-spin stabilities due to one-centered exchange integrals had interesting maxima when the magnitude of intra- and intermolecular resonance integrals

was nearly equal. The physical meanings of these maxima were also clarified by analyzing the orbital patterns of localized NBMOs. Our analysis was supported by quantum chemical calculations including the electron correlation.

Theoretical

We express the i-th and j-th NBMOs as follows:

$$\phi_i = \sum_r C_{ri}\chi_r \tag{2}$$

$$\phi_j = \sum_s C_{sj}\chi_s \tag{3}$$

where C_{ri} and C_{sj} are Hückel-molecular-orbital coefficients on the carbon atomic sites r and s in NBMO ϕ_i and ϕ_j, respectively. χ represents $2p_z$ carbon atomic orbitals. The summation includes all carbon atomic sites. For convenience, we define the product of NBMOs (PNBMOs) as effective two electron wave function:[1,18]

$$\begin{aligned} PNBMO_{i,j} = \phi_i(\mathbf{1})\phi_j(\mathbf{2}) &= \sum_r \sum_s C_{ri}C_{sj}\chi_r(\mathbf{1})\chi_s(\mathbf{2}) \\ &\cong C\sum_r C_{ri}C_{rj}\chi_r(\mathbf{1})\chi_r(\mathbf{2}) \end{aligned} \tag{4}$$

where the differential overlaps were neglected in the approximation (NDO approximation). The electron numbers **1** and **2** were added for clarity. The NDO approximation is adequate for the present purpose, because the exchange integral between NBMOs results from ionic terms, in which simultaneous occupation of two electrons with parallel spins is forbidden. The exchange integral between a certain pair of NBMOs is as follows:

$$\begin{aligned} K_{ij} &= \iint \phi_i(\mathbf{1})\phi_j(\mathbf{1})\frac{e^2}{r_{12}}\phi_i(\mathbf{2})\phi_j(\mathbf{2})\mathrm{d}\tau_1\mathrm{d}\tau_2 \\ &= \sum_r\sum_s\sum_t\sum_u C_{ri}C_{sj}C_{ti}C_{uj}(rs|tu) \\ &\cong \sum_r {C_{ri}}^2{C_{rj}}^2(rr|rr) \propto \sum_r {C_{ri}}^2{C_{rj}}^2 = L_{ij} \end{aligned} \tag{5}$$

where $(rs|tu)$ is the electron-repulsion integral and only one-centered integrals were taken into account.[15–17] L_{ij} is a non-dimensional index approximately proportional to the exchange integral, which has been introduced by Aoki and Imamura.[15] From eqs 2–4, we see that the L_{ij} index is identical to the square of norm in PNBMOs, that is, sum of the squared amplitudes of PNBMOs. Therefore, simple products between the coefficients on the same carbon atomic site of each NBMO become $C_{ri}C_{rj}$, and the sum of their square ${C_{ri}}^2{C_{rj}}^2$ is approximately proportional to the exchange integral. Therefore, we can estimate the exchange integral by amplitude patterns of the PNBMOs, and the origin of high-spin stabilities in organic-radical assemblies is schematically deduced. In our treatment, the intermolecular distance is not a constant but a variable. Therefore, we need to extend the usual NBMO method taking account of the variable resonance integral. The procedure to obtain the NBMOs is explained as follows by analyzing allyl, pseudo-*para*-benzyl, and pseudo-*ortho*-benzyl dimers.

Allyl-Radical Dimers. As described in our previous work,[1] topological linkage of carbon atomic sites of ally-radical dimer **1** is similar to non-Kekulé biradical 1,3-dimethylenecyclobutadiene (**8**) as described in Figure 5. Therefore, we can perform Hückel-like molecular orbital analysis on **1** by focusing only on the topological linkage, as described below.

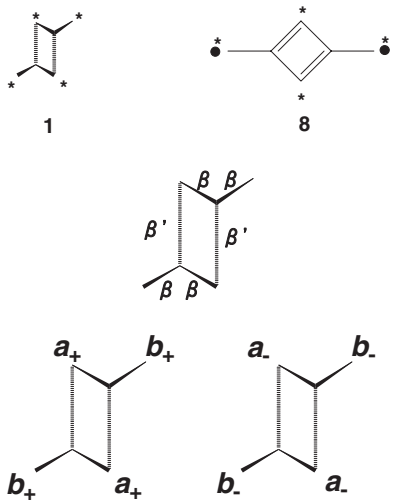

Figure 5. Structural resemblance between **1** and 1,3-dimethylenecyclobutadiene (**8**). Definition of resonance integrals and NBMO coefficients of **1** is also shown.

The NBMOs are obtained by solving the corresponding Hückel secular equation. In alternate hydrocarbons such as the present cases, the carbon atomic sites are divided into two groups, that is, starred atoms and unstarred atoms, which are not adjacent to each other. Then, the secular equation is equivalent to the following:

$$xC_{ri} + \sum_{s=R+1}^{N}\gamma_{rs}C_{si} = 0$$
$$\text{(for starred-atoms row; } r = 1, 2, \ldots, R) \tag{6}$$

$$xC_{ri} + \sum_{s=1}^{R}\gamma_{rs}C_{si} = 0$$
$$\text{(for unstarred-atoms row; } r = R+1, \ldots, N) \tag{7}$$

where x is:

$$x = \frac{\alpha - \varepsilon}{\beta_{rs}} \tag{8}$$

α is the Coulomb integral. β_{rs} is the resonance integral between the r-th and s-th sites. ε is orbital energy. In eqs 6 and 7, N is the number of carbon atomic sites. R is the number of starred atoms, and thus, $(N-R)$ becomes the number of unstarred atoms. γ_{rs} is resonance-integral ratio based on a standard value, as explained below.

As shown in Figure 5, intramolecular resonance integrals are considered to have the same value β, similar to usual π systems. When we take account of parallel translation, intermolecular resonance integrals are also considered to have the same value β'. Therefore, when we regard β as a standard value, γ_{rs} becomes:

$$\begin{aligned} &\gamma_{rs} = 1 \quad \text{(intramolecular)}, \\ &\gamma_{rs} = \frac{\beta'}{\beta} = \gamma = \text{const.} \ \text{(intermolecular)} \end{aligned} \tag{9}$$

When $x = 0$, we obtain NBMOs. C_{ri} on unstarred atoms are all zero, because $R > (N - R)$.[21] C_{ri} on starred atoms satisfy the following extended "zero sum rule:"

$$\sum_{s=1}^{R} \gamma_{rs} C_{si} = 0 \quad \text{(for starred atoms; } r = 1, 2, \ldots, R) \quad (10)$$

We note that the number of NBMOs is the difference between the number of starred atoms and unstarred atoms, that is, $\{R - (N - R)\} = 2R - N$. The number of formal Kekulé double bonds T becomes $(N - R)$, and thus, the number of NBMOs is $(N - 2T)$, analogous to non-Kekulé planar molecules.[21] In the present dimers, there exists two NBMOs.

Now we consider intermolecular distance dependence on the NBMOs coefficients. β' is approximately proportional to the overlap integral between the adjacent intermolecular sites, as is supposed in extended Hückel method.[22] Then, γ decreases with the intermolecular distance d, because the overlap integral decreases with d.

When the NBMO coefficients of **1** are tentatively denoted as a and b (Figure 5), two independent solutions corresponding to spatial symmetry and antisymmetry are obtained. That is,

$$a_{\pm} = \frac{1}{\sqrt{2}\sqrt{\gamma^2 \pm 2\gamma + 2}}, \quad b_{\pm} = -\frac{1 \pm \gamma}{\sqrt{2}\sqrt{\gamma^2 \pm 2\gamma + 2}} \quad (11)$$

where plus and minus signs correspond to the symmetry and antisymmetry with respect to the inversion operation.

Then, from eq 5, the exchange integral K_{ij} between the two independent NBMOs is approximately proportional to dimensionless quantity L_{ij} as follows:

$$\begin{aligned} K_{ij} &\propto 2(a_+)^2(a_-)^2 + 2(b_+)^2(b_-)^2 \\ &= \frac{1}{2}\frac{1 + (\gamma^2 - 1)^2}{(\gamma^2 + 2\gamma + 2)(\gamma^2 - 2\gamma + 2)} = L_{ij} \end{aligned} \quad (12)$$

In the present dimers, K_{ij} should be proportional to the triplet–singlet energy gap.

The resonance integral parameter γ increases when the intermolecular distance d decreases, and vice versa. Therefore, in order to grasp the intermolecular distance dependence of the high-spin stabilities, it is convenient to plot the L_{ij} index versus $1/\gamma$. The $1/\gamma$ dependence on L_{ij} of **1** is shown in Figure 6a. L_{ij} increases when $1/\gamma \to 0$ and $1/\gamma \to \infty$. This is physically unreasonable. In particular, the triplet–singlet energy gap ($\propto L_{ij}$) should be zero when the intermolecular distance becomes infinity. Therefore, we transformed the two NBMOs so as to minimize L_{ij}. This procedure was done as follows.

The two NBMOs of **1** obtained above were transformed by unitary matrix, which has been introduced by Aoki and Imamura:[15]

$$\begin{pmatrix} \psi_i \\ \psi_j \end{pmatrix} = \begin{pmatrix} \sin\theta & \cos\theta \\ -\cos\theta & \sin\theta \end{pmatrix} \begin{pmatrix} \phi_i \\ \phi_j \end{pmatrix} \quad (13)$$

θ serves as an orbital mixing parameter. Then, θ dependence on the exchange integral K_{ij} is:

$$\begin{aligned} K_{ij} &\propto |PNBMO_{i,j}|^2 \propto L_{ij} \\ &= \sum_r (C'_{ri} C'_{rj})^2 = \frac{1}{8}(\alpha_{ij} + 4\beta_{ij}) - A\sin(4\theta + \varphi) \end{aligned} \quad (14)$$

where C'_{ri} and C'_{rj} are new coefficients of the NBMOs ψ_i and ψ_j after the unitary transformation. Again, L_{ij} is the Aoki–Imamura index, which should be minimized.[15] The first and second terms on the right are related each other by the following eqs 15–19:[15]

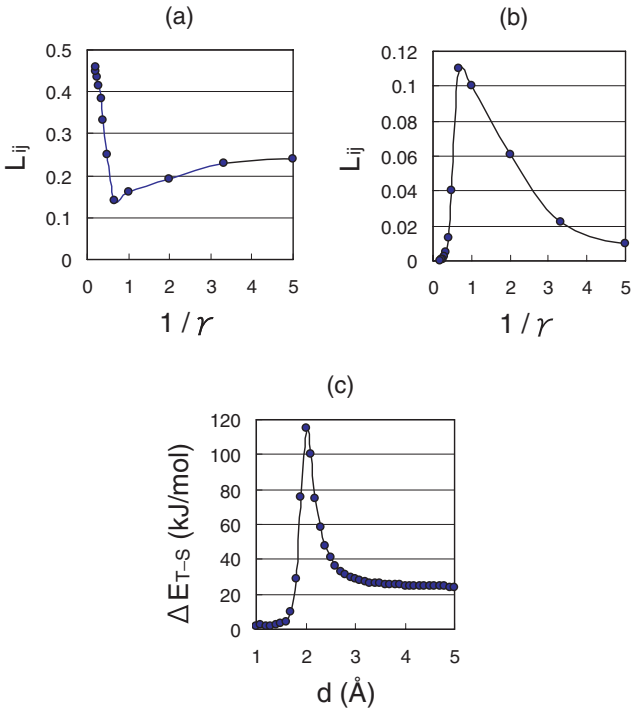

Figure 6. Intermolecular-distance dependences on L_{ij} index in **1**. (a) Before unitary transformation, (b) after unitary transformation, and (c) theoretical calculation on ΔE_{T-S} at PM3-CI level of theory.

$$\pm A = \frac{1}{2}\sqrt{{\gamma_{ij}}^2 + \frac{1}{16}(\alpha_{ij} - 4\beta_{ij})^2} \quad (15)$$

$$\varphi = \tan^{-1}\frac{\alpha_{ij} - 4\beta_{ij}}{4\gamma_{ij}} \quad (16)$$

$$\alpha_{ij} = \sum_r ({C_{rj}}^2 - {C_{ri}}^2)^2 \quad (17)$$

$$\beta_{ij} = \sum_r {C_{ri}}^2 {C_{rj}}^2 \quad (18)$$

$$\gamma_{ij} = \sum_r ({C_{rj}}^2 - {C_{ri}}^2) C_{ri} C_{rj} \quad (19)$$

If A is positive, L_{ij} is minimized when

$$4\theta + \varphi = \frac{\pi}{2} \quad (20)$$

Thus, the parameter θ which leads to the minimal exchange integral is given by eq 21:

$$\theta = \frac{1}{4}\left(\frac{\pi}{2} - \varphi\right) \quad (21)$$

The unitary-transformed NBMOs described above are spatially localized to each other as much as possible.

The intermolecular distance dependence on unitary-transformed L_{ij} is plotted in Figure 6b. The global behavior of the graph is very interesting in that there exists a maximum at $1/\gamma \fallingdotseq 0.7$. That is, there exists an optimum distance for the high-spin stability in **1**, and the optimum is realized when the magnitude of the intra- and intermolecular resonance integrals

are nearly equal. This is not deduced from conventional UHF analysis on organic assemblies, because UHF is rationalized to the simple spin-polarization model.[4–6] In addition, when the intermolecular distance is large ($1/\gamma \to \infty$), L_{ij} decreased and converged to zero. This is quite reasonable, because the triplet–singlet energy gap should decrease with intermolecular distance due to localization of NBMOs. Such a decrease of the exchange integral at large intermolecular distances is consistent with earlier UHF studies of organic-radical dimers.[6]

However, in order to confirm such behaviors including the optimum for high-spin stability, it is necessary to perform quantum chemical calculations on triplet–singlet energy gap $\Delta E_{\text{T–S}}$, which is equal to the exchange integral. For our purposes, qualitative rather than quantitative description should be emphasized, because amplitude patterns in NBMOs are not so sensitive to level of theory. Thus, we calculated $\Delta E_{\text{T–S}}$ at PM3 level of theory[23] including configuration interaction (CI) by using semi-empirical molecular orbital program MOPAC2000.[24] CI method is suitable for calculations of degenerate systems, especially in low-spin states, which cannot be well described with one Slater determinant.[25] In addition, CI method is appropriate to our purpose, because electronic correlation is invaluable to describe electronic states of supermolecules separated by large distance. CI wave functions are convenient for description of open-shell systems, because they satisfy spin symmetries. The active space for CI was spanned by four electrons and four orbitals including the NBMOs within the ROHF (restricted open Hartree–Fock) reference configurations. The calculation was done with CAS (complete active space) method.

Figure 6c is the calculated $\Delta E_{\text{T–S}}$ curve versus the intermolecular distance d. When $d \fallingdotseq 2.0$ Å, $\Delta E_{\text{T–S}}$ was maximized. That is, there exists an optimum point for the high-spin stability, consistent with the theoretical curve in Figure 6b. When $d \to 0$ and $d \to \infty$, $\Delta E_{\text{T–S}}$ converged to zero. This is also reasonable. The physical meaning of such behaviors is discussed later in detail.

Benzyl-Radical Dimers. Next, we analyze benzyl radical dimers as further examples of organic-radical assemblies. Experimentally, pseudo-*para*- and pseudo-*ortho*-cyclophane-bridged derivatives were synthesized and their high-spin stabilities have been established by ESR measurements.[7–9] Therefore, benzyl dimers are good models for theoretical analysis on these experimental results. Similar to the allyl dimer, we obtained two NBMOs by the corresponding secular equation, and they were localized by the unitary-transformation procedure.

We first analyzed pseudo-*para*-benzyl dimer **2**. Definition of the resonance integrals is shown in Figure 7. When the NBMO coefficients are tentatively denoted as a, b, and c as described in Figure 7, two independent solutions of the NBMOs become:

$$a_\pm = \frac{\gamma^2 \pm \gamma - 2}{\sqrt{2}\sqrt{\gamma^4 \pm 2\gamma^3 - 2\gamma^2 \mp 2\gamma + 7}},$$
$$b_\pm = \frac{1}{\sqrt{2}\sqrt{\gamma^4 \pm 2\gamma^3 - 2\gamma^2 \mp 2\gamma + 7}},$$
$$c_\pm = -\frac{1 \pm \gamma}{\sqrt{2}\sqrt{\gamma^4 \pm 2\gamma^3 - 2\gamma^2 \mp 2\gamma + 7}} \tag{22}$$

where signs of the subscripts correspond to symmetry (+) and

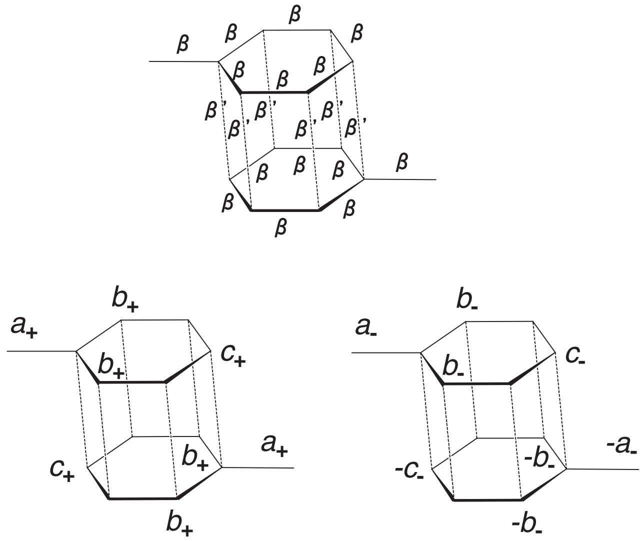

Figure 7. Definition of resonance integrals and NBMO coefficients of pseudo-*para*-benzyl dimer **2**.

antisymmetry (−) with respect to the inversion. The exchange integral becomes:

$$K_{ij} \propto 2(a_+)^2(a_-)^2 + 4(b_+)^2(b_-)^2 + 2(c_+)^2(c_-)^2$$
$$= \frac{1}{2}\frac{(\gamma^2+\gamma-2)^2(\gamma^2-\gamma-2)^2 + 2 + (\gamma+1)^2(\gamma-1)^2}{(\gamma^4+2\gamma^3-2\gamma^2-2\gamma+7)(\gamma^4-2\gamma^3-2\gamma^2+2\gamma+7)}$$
$$= L_{ij} \tag{23}$$

Figure 8a is plot of the L_{ij} index versus $1/\gamma$ before the unitary transformation. The curve is physically unreasonable, because the exchange integral increases with dissociation of two benzyl moieties. On the other hand, after unitary transformation, the L_{ij} index showed interesting behavior with a maximum, qualitatively similar to the allyl dimer as depicted in Figure 8b. That is, the high-spin stability has a maximum with $1/\gamma \fallingdotseq 0.5$. The second maxima at $1/\gamma \fallingdotseq 2$ results from another zero point in the differential form of eq 23. The second maxima, however, seems not so important, because this is probably due to the complex γ- and θ-dependence on L_{ij} index. Anyway, there exists at least one high-spin optimum. The existence of the high-spin optimum is interesting not only theoretically but also from a molecular-engineering point of view. The theoretical plot was confirmed by CI calculation, similar to the allyl-radical dimer. Figure 8c is the calculated high-spin stability $\Delta E_{\text{T–S}}$ at the PM3-CI level of theory. The optimum of $\Delta E_{\text{T–S}}$ appeared at the distance $d \fallingdotseq 2.0$ Å. When $d > 2.0$ Å, $\Delta E_{\text{T–S}}$ decreased from ca. 100 kJ mol^{-1} to zero, qualitatively consistent with the UHF study by Yamaguchi et al.[6] Experimentally, high-spin carbene dimer **3** has intermolecular distance $d \fallingdotseq 3.0$ Å, which results from the cyclophane bridge. From ESR studies, **3** has been characterized as a ground-state quintet molecule due to the two carbene moieties. Apart from the additional σ-type electrons, pseudo-*para*-benzyl dimer is considered to be a good model for **3**, because NBMO–NBMO interactions occur within the face-to-face-stacked π plains.

Next, pseudo-*ortho*-benzyl dimer was similarly analyzed referring to Figure 9. When the NBMO coefficients are

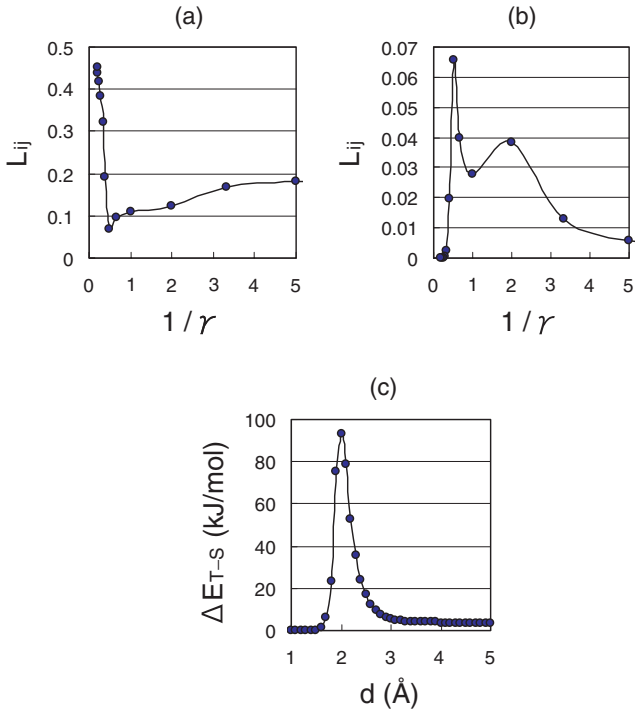

Figure 8. Intermolecular-distance dependences on L_{ij} index in pseudo-*para*-benzyl dimer **2**. (a) Before unitary transformation, (b) after unitary transformation, and (c) theoretical calculation on ΔE_{T-S} at PM3-CI level of theory.

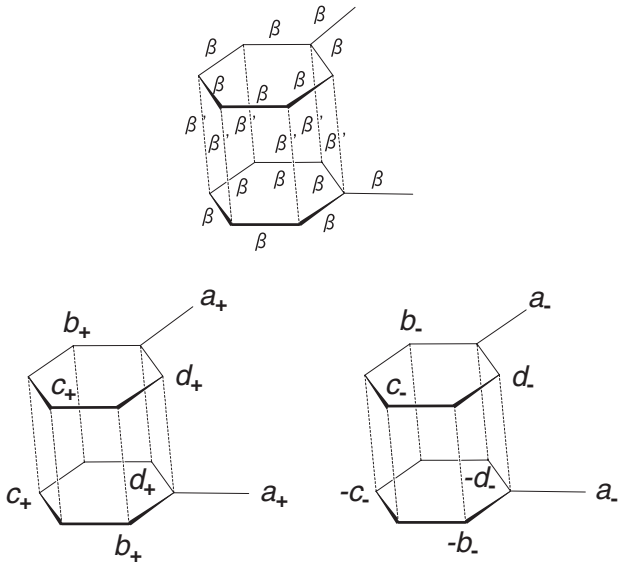

Figure 9. Definition of resonance integrals and NBMO coefficients of pseudo-*ortho*-benzyl dimer **4**.

tentatively denoted as a, b, c, and d as described in Figure 9, two independent solutions of the NBMOs become:

$$a_\pm = \frac{\mp\gamma^3 - 2\gamma^2 \pm \gamma + 2}{\sqrt{2}\sqrt{\gamma^6 \pm 4\gamma^5 + 3\gamma^4 \mp 6\gamma^3 - 7\gamma^2 \pm 4\gamma + 7}},$$

$$b_\pm = -\frac{1 \pm \gamma}{\sqrt{2}\sqrt{\gamma^6 \pm 4\gamma^5 + 3\gamma^4 \mp 6\gamma^3 - 7\gamma^2 \pm 4\gamma + 7}},$$

$$c_\pm = \frac{1}{\sqrt{2}\sqrt{\gamma^6 \pm 4\gamma^5 + 3\gamma^4 \mp 6\gamma^3 - 7\gamma^2 \pm 4\gamma + 7}},$$

$$d_\pm = \frac{\gamma^2 \pm \gamma - 1}{\sqrt{2}\sqrt{\gamma^6 \pm 4\gamma^5 + 3\gamma^4 \mp 6\gamma^3 - 7\gamma^2 \pm 4\gamma + 7}} \quad (24)$$

where signs of the coefficients correspond to the symmetric (+) and antisymmetric (−) characters with respect to the rotation. The exchange integral becomes:

$$\begin{aligned} K_{ij} &\propto 2(a_+)^2(a_-)^2 + 2(b_+)^2(b_-)^2 + 2(c_+)^2(c_-)^2 + 2(d_+)^2(d_-)^2 \\ &= \frac{1}{2}\frac{1}{(\gamma^6 + 4\gamma^5 + 3\gamma^4 - 6\gamma^3 - 7\gamma^2 + 4\gamma + 7)(\gamma^6 - 4\gamma^5 + 3\gamma^4 - 6\gamma^3 - 7\gamma^2 + 4\gamma + 7)} \\ &\quad \times \{(-\gamma^3 - 2\gamma^2 + \gamma + 2)^2(-\gamma^3 - 2\gamma^2 + \gamma + 2)^2 + (\gamma + 1)^2(\gamma - 1)^2 + 1 + (\gamma^2 + \gamma - 1)^2(\gamma^2 - \gamma - 1)^2\} = L_{ij} \end{aligned} \quad (25)$$

A theoretical curve for the L_{ij} index before unitary transformation is plotted in Figure 10a. The qualitative behavior is similar to the pseudo-para dimer. After unitary transformation, the L_{ij} index was minimized, as shown in Figure 10b. As a result, there appeared a maximum point, similar to the pseudo-para dimer. The high-spin stability was optimized at $1/\gamma \fallingdotseq 1$. This is also an interesting phenomenon due to the orbital mixing, in which localization of NBMOs and the corresponding exchange integral are optimized. PM3-CI calculation of the ΔE_{T-S} was also done, and plotted versus d in Figure 10c. The high-spin stability was optimized at $d \fallingdotseq 1.8$ Å.

Thus, in organic-radical assemblies, we have shown that there exists high-spin-stability optimum with respect to the intermolecular distance. As a whole, the optimum are realized when magnitude of intra- and intermolecular resonance integrals is nearly equal, that is, $1/\gamma \fallingdotseq 1$. In the next section, we clarify the origin of the optimum by analyzing the relationship between amplitude patterns of localized NBMOs and exchange integrals.

Discussion

The origin of the optimum for the high-spin stability in organic-radical assemblies is deduced by analyzing the intermolecular-distance dependence on amplitude patterns of NBMOs. We examine the amplitude patterns in large, moderate, and small intermolecular-distance regions.

The amplitude patterns of NBMOs in allyl-radical dimer **1** are depicted in Figure 11. The patterns are schematically depicted for selected intermolecular-distance d. The corresponding parameter $1/\gamma$ is also noted. As shown in the top of Figure 11, when two allyl-radical moieties are infinitely separated, that is, $d \to \infty$ ($1/\gamma \to \infty$), two NBMOs before the unitary transformation are canonical orbitals. They are delocalized as much as possible. Then, the exchange integral

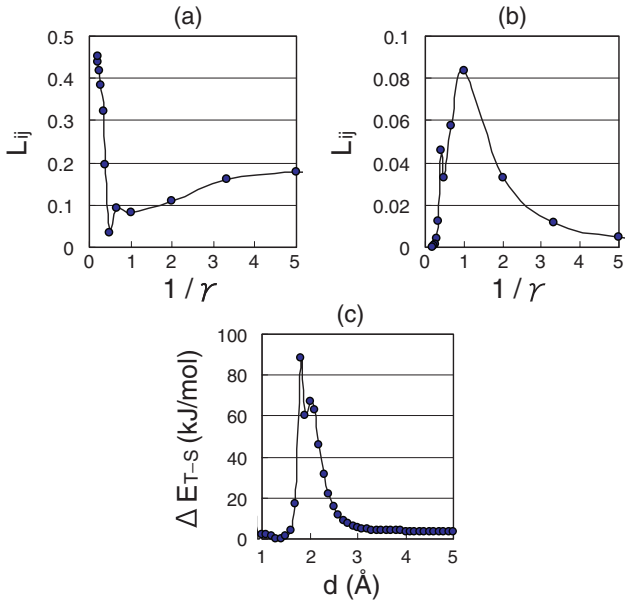

Figure 10. Intermolecular-distance dependences on L_{ij} index in pseudo-*ortho*-benzyl dimer **4**. (a) Before unitary transformation, (b) after unitary transformation, and (c) theoretical calculation on ΔE_{T-S} at PM3-CI level of theory.

has positive value, because the NBMOs span common atoms. After the unitary transformation, two NBMOs become completely disjoint allyl-radical NBMOs, which are spatially separated as much as possible. They are localized NBMOs. Then, the exchange integral becomes zero, because the NBMOs do not span common atoms. Thus, when $d \to \infty$, unitary transformation minimizes the exchange integral so that the NBMOs are completely localized each other. In other word, unitary transformation is essential to describe the triplet–singlet energy gap ΔE_{T-S} correctly, because ΔE_{T-S} should converge to zero when $d \to \infty$.

When d has intermediate value, unitary transformation gives a positive exchange integral. For example, when $d \fallingdotseq 2$ Å ($1/\gamma \fallingdotseq 1$), the NBMOs of **1** are not completely separated from each other, but delocalized at common atoms both before and after the unitary transformation. This is schematically illustrated for $1/\gamma = 1$ in the middle of Figure 11. Before the unitary transformation, each NBMO is canonical in that the spatial symmetries are satisfied. After the unitary transformation, each NBMO is also canonical, because the unitary-transformation parameter θ is zero. The exchange integral is not zero, because the NBMOs are nondisjoint, which span common atoms. That is, the one-centered exchange integral resulting from eq 5 always has a positive value due to the common spanned atomic orbitals. This situation resembles that in non-Kekulé planar molecules, which are classified into

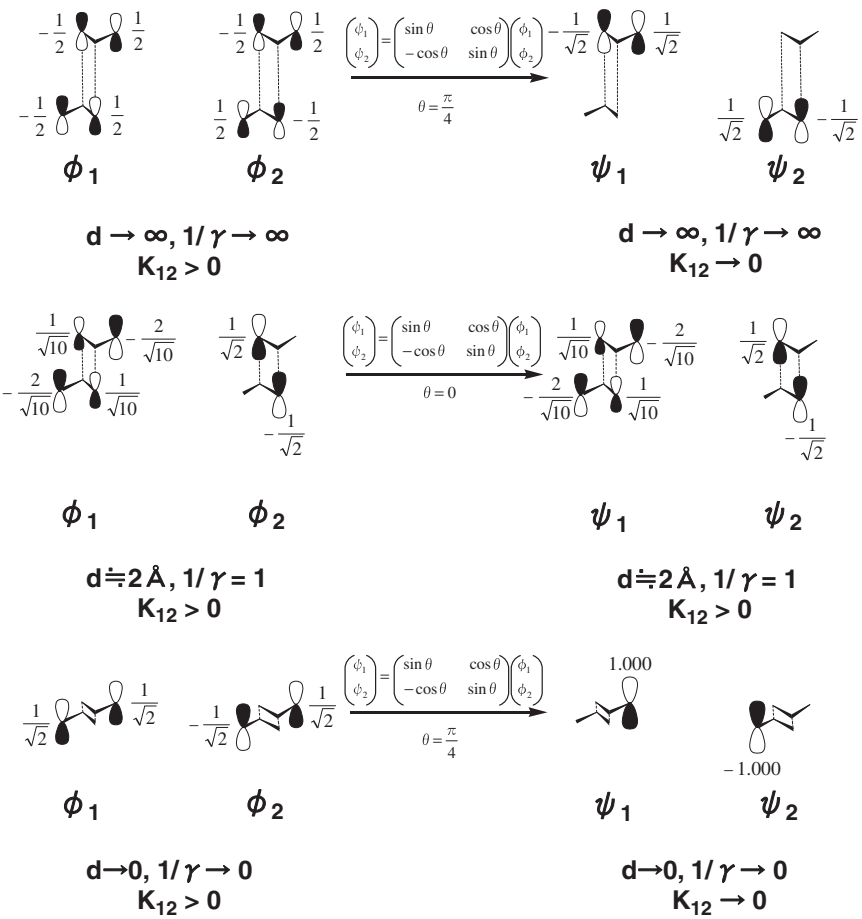

Figure 11. Amplitude-pattern dependences on exchange integrals in **1**.

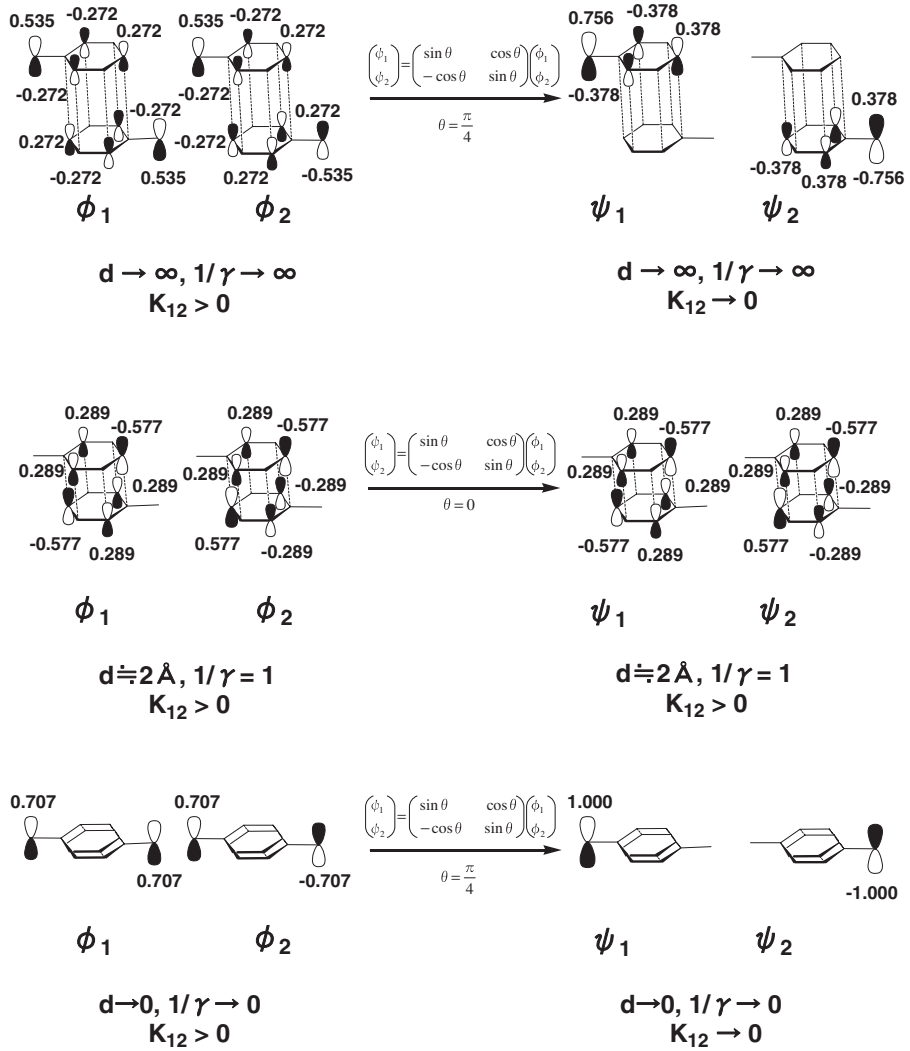

Figure 12. Amplitude-pattern dependences on exchange integrals in **2**.

two groups, that is, disjoint and nondisjoint groups. The NBMOs of nondisjoint systems span common atoms. As a result, they always have positive exchange integrals due to the common spanned atomic orbitals. The common spanned atomic orbitals are expressed by ionic terms $\chi_r(\mathbf{1})\chi_r(\mathbf{2})$, and the corresponding squared amplitudes become $C_{ri}{}^2C_{rj}{}^2$, as seen from eq 4. The ionic terms mean simultaneous occupancy of two electrons in the same atomic orbital. Since the Pauli principle inhibits simultaneous occupation of two electrons with parallel spins, Coulomb repulsions between two electrons in the antiparallel-spin state are larger than those in the parallel-spin states. Therefore, the ionic terms lead to high-spin states. Thus, in organic-radical assemblies separated by intermediate distance, any unitary transformation gives positive exchange integrals.

When $d \to 0$ $(1/\gamma \to 0)$, unitary transformation makes the positive exchange integral zero. For example, we consider an extreme case with $d = 0$ $(1/\gamma = 0)$ referring to the bottom of Figure 11. Before unitary transformation, the NBMOs of **1** span common atoms at the terminal methylene carbons, and lead to a positive exchange integral. On the other hand, after unitary transformation, the NBMOs span no common atoms. The NBMOs separately spread at each methylene carbon. This is disjoint character, similar to low-spin biradicals.[13] Therefore, the exchange integral should be zero. Although such a situation is an extremity of theory, the disjoint character guarantees the high-spin optimum.

Thus, when d is extremely small or large, the NBMOs are disjoint, of which exchange integrals are zero. On the other hand, when d has moderate values ($d \fallingdotseq 2$ Å, $1/\gamma \fallingdotseq 1$), the NBMOs become nondisjoint, of which the exchange integral is positive. This is the origin of the optimum in the high-spin stability. The orbital-pattern analysis described above is consistent with the theoretical curve of the L_{ij} index, as described in Figure 6.

Benzyl-radical dimers can be also analyzed by the same method. The amplitude patterns of pseudo-*para*-benzyl dimer are shown in Figure 12. When $d \to \infty$ $(1/\gamma \to \infty)$ or $d \to 0$ $(1/\gamma \to 0)$, the NBMOs are essentially disjoint, because unitary transformation makes the NBMOs spatially separate. The exchange integrals should be zero. On the other hand, when d has moderate values, the NBMOs become nondisjoint. For example, $d \fallingdotseq 2$ Å $(1/\gamma \fallingdotseq 1)$, both before and after the unitary transformation, the NBMOs span common atoms,

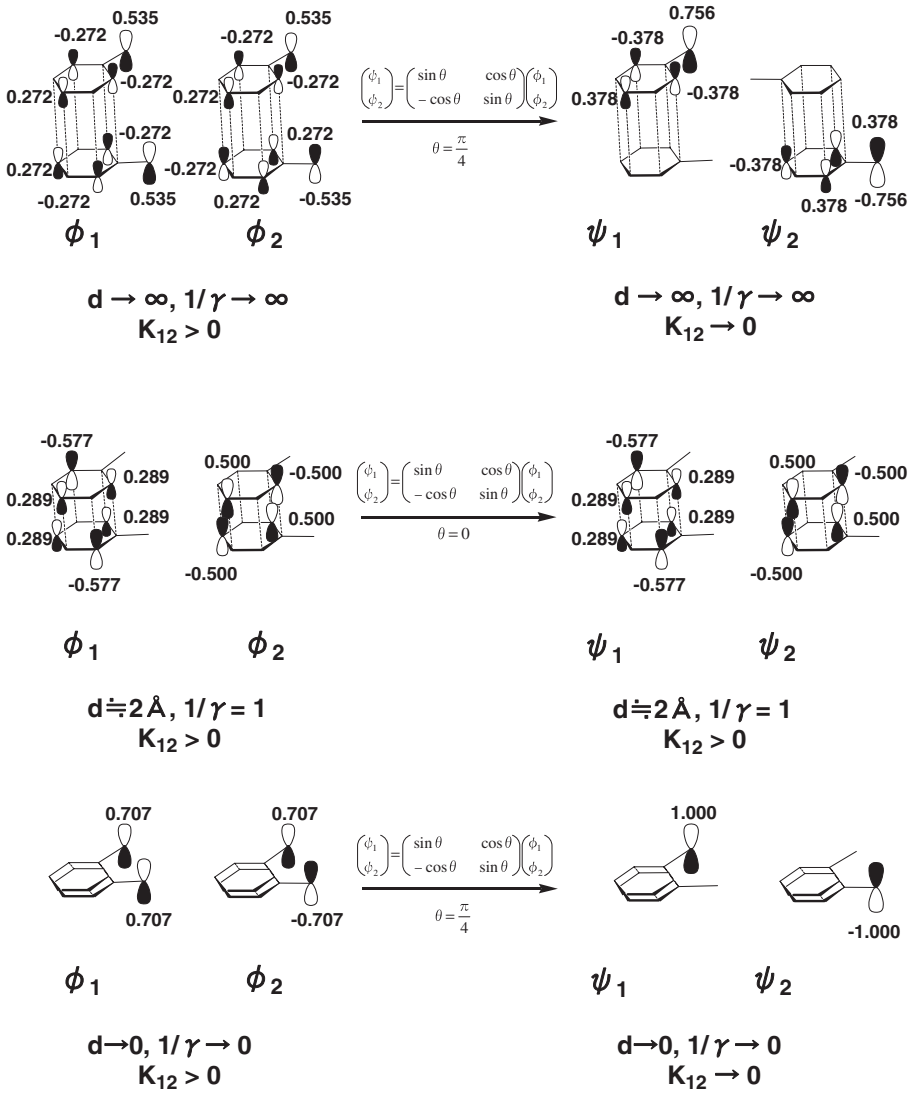

Figure 13. Amplitude-pattern dependences on exchange integrals in **4**.

which lead to positive exchange integral. This is origin of the optimum in the high-spin stability.

Similarly, the amplitude patterns of pseudo-*ortho*-benzyl dimer are shown in Figure 13. When $d \to \infty$ or $d \to 0$, the NBMOs are essentially disjoint, and the exchange integral is zero. On the other hand, when d has moderate values, the NBMOs become nondisjoint. When $d \fallingdotseq 2$ Å, both before and after the unitary transformation, the NBMOs span common atoms, and thus, exchange integral is positive. This is the origin of the optimum in the high-spin stability.

Thus, in organic-radical assemblies, there exists an optimum for the high-spin stability with respect to the intermolecular distance. The origin of the optimum is attributed to disjoint character in small and large intermolecular distance region and nondisjoint character in moderate intermolecular distance region. The optimum resulted from unitary transformation of NBMOs, and theoretical plot of the exchange integral was confirmed by quantum chemical calculations. Since our method is based on molecular orbital method, the ionic terms create one centered exchange integrals. Therefore, high-spin stabilities are considered to be originated from Coulomb repulsions on the common-spanned atomic orbitals. The non-bonding electrons are not localized only at one radical moiety, but delocalized over two radical moieties. Such itinerant character of non-bonding electrons causes positive exchange integrals, of which the main contribution is one center Coulomb repulsion.

Conclusion

Intermolecular distance dependence on ferromagnetic interactions in organic-radical assemblies was deduced by using molecular orbital methods. It was shown that non-bonding molecular orbitals (NBMOs) were subject to orbital mixing to form localized NBMOs. In small and large intermolecular distance regions, NBMOs were spatially separated from each other. On the other hand, in moderate intermolecular distance regions, NBMOs were spread over common atoms. As a result, high-spin stabilities due to the exchange integrals between NBMOs had maxima when magnitude of intra- and intermolecular resonance integrals was nearly equal. In the moderate intermolecular distance regions, the non-bonding electrons had highly itinerant character. Our analysis was supported by quantum-chemical calculations.

References

1 First communication: M. Hatanaka, R. Shiba, *Bull. Chem. Soc. Jpn.* **2008**, *81*, 966.
2 H. M. McConnell, *J. Chem. Phys.* **1963**, *39*, 1910.
3 A. A. Ovchinnikov, *Theor. Chim. Acta* **1978**, *47*, 297.
4 K. Yamaguchi, T. Fueno, *Chem. Phys. Lett.* **1989**, *159*, 465.
5 K. Yamaguchi, Y. Toyoda, T. Fueno, *Chem. Phys. Lett.* **1989**, *159*, 459.
6 K. Yamaguchi, H. Namimoto, T. Fueno, *Mol. Cryst. Liq. Cryst.* **1989**, *176*, 151.
7 A. Izuoka, S. Murata, T. Sugawara, H. Iwamura, *J. Am. Chem. Soc.* **1985**, *107*, 1786.
8 A. Izuoka, S. Murata, T. Sugawara, H. Iwamura, *J. Am. Chem. Soc.* **1987**, *109*, 2631.
9 H. Iwamura, *Adv. Phys. Org. Chem.* **1990**, *26*, 179.
10 K. Tanaka, T. Takeuchi, K. Yoshizawa, M. Toriumi, T. Yamabe, *Synth. Met.* **1991**, *44*, 1.
11 K. Yoshizawa, R. Hoffmann, *J. Am. Chem. Soc.* **1995**, *117*, 6921.
12 K. Yoshizawa, T. Yamabe, R. Hoffmann, *Mol. Cryst. Liq. Cryst.* **1997**, *305*, 157.
13 W. T. Borden, E. R. Davidson, *J. Am. Chem. Soc.* **1977**, *99*, 4587.
14 W. T. Borden, *Mol. Cryst. Liq. Cryst.* **1993**, *232*, 195.
15 Y. Aoki, A. Imamura, *Int. J. Quantum Chem.* **1999**, *74*, 491.
16 Y. Orimoto, T. Imai, K. Naka, Y. Aoki, *J. Phys. Chem. A* **2006**, *110*, 5803.
17 Y. Orimoto, Y. Aoki, *J. Chem. Theory Comput.* **2006**, *2*, 786.
18 M. Hatanaka, R. Shiba, *Bull. Chem. Soc. Jpn.* **2007**, *80*, 1750.
19 M. Hatanaka, R. Shiba, *Bull. Chem. Soc. Jpn.* **2007**, *80*, 2342.
20 M. Hatanaka, R. Shiba, *Bull. Chem. Soc. Jpn.* **2008**, *81*, 460.
21 H. C. Longuet-Higgins, *J. Chem. Phys.* **1950**, *18*, 265.
22 R. Hoffmann, *J. Chem. Phys.* **1963**, *39*, 1397.
23 J. J. P. Stewart, *J. Comput. Chem.* **1989**, *10*, 209.
24 J. J. P. Stewart, *MOPAC2000 in Chem3D, Ultra version 8.0*, CambridgeSoft.
25 M. Hatanaka, R. Shiba, *J. Comput. Chem. Jpn.* **2006**, *5*, 171.